

## Supporting Information

### **Large-scale, ultrahigh-resolution nanoemitter ordered array with PL brightness enhanced by PEALD-grown AlN coating**

**Mingzeng Peng,\* Xinhe Zheng,\* Sanjie Liu, Huiyun Wei, Yingfeng He, Meiling Li, Yunlai An, Yimeng Song, Peng Qiu**

Beijing Key Laboratory for Magneto-Photoelectrical Composite and Interface Science, School of Mathematics and Physics, University of Science and Technology Beijing, No. 30, Xueyuan Road, Beijing 100083, China

\*Address correspondence to [mzpeng@ustb.edu.cn](mailto:mzpeng@ustb.edu.cn) (MZP), [xinhezhen@ustb.edu.cn](mailto:xinhezhen@ustb.edu.cn)

### **Contents**

#### **1. Increasing pixel density of InGaN/GaN MQW pillar ordered array for ultrahigh-resolution display**

Based on the nanometer-level patterning and top-down etching, we can further reduce the three-dimensional size of InGaN/GaN MQW pillar array in state of the art. Fig. S1 presents four pillar arrays with different pixel densities of  $6.25 \times 10^6$ ,  $9.59 \times 10^6$ ,  $2.5 \times 10^7$ ,  $1.56 \times 10^8$   $\text{cm}^{-2}$ , respectively. The pixel diameter has been decreased from  $>1$   $\mu\text{m}$  to 200 nm level, which gradually approaches to the optical wavelength. As shown in Fig. S1d, the newly-developed nanometer-level array with a smallest diameter of  $\sim 200$  nm has achieved a much higher pixel density of  $1.56 \times 10^8$   $\text{cm}^{-2}$ , which increases about 25 folds with regard to the early-fabricated micro-array in Fig. S1a. As a result, it is beneficial to greatly improve the pixel resolution for high-end display or imaging applications.

#### **2. Geometrical structure on the PL characteristic of 3D nanoemitter**

The PL property of unpassivated InGaN/GaN MQW nanoemitter is directly dependent on its geometrical structure. In our experiment, we choose its length or height around 1.5~2  $\mu\text{m}$  controlled by top-down etching down to n-type GaN

underlayer, which guarantees that the luminous regions of different nanoemitter pixels are completely separated from each other. In this case, the luminous region of each nanoemitter is unchanged despite of its different lengths or heights. It is mainly dependent on its diameter and density, which hence determined the effective luminous area for PL emission.

On the one hand, the average PL intensity of single nanemitter has been determined from dividing the total PL power by the array density. As shown in Fig. S2, its average PL intensity decreases rapidly as the reduction of its diameter. The smaller the single nanoemitter, the lower PL intensity it has. On the other hand, considering the shrinkage of luminous area induced by diameter, the PL intensity per unit area (or effective PL density) of different nanoemitter arrays has been evaluated in Fig. S2. It changes little in the diameter range of 0.8~1.2  $\mu\text{m}$  while decreases obviously in the smaller diameters. The PL performance has been partially influenced by decreasing the pixel diameter or size at sub-micrometer level. It demonstrates that the higher surface-volume ratio of 3D nanoemitter plays a great role on its effective PL performance. So the surface passivation is indispensably needed to achieve its high PL brightness.

### **3. The coverage of AlN coating layer around nanoemitter ordered array**

The PEALD-grown AlN layer was implemented to passivate the sidewall of the InGaN/GaN MQW nanoemitter ordered array. The coverage of AlN coating layer is taken into consideration to evaluate its uniform and conformal deposition around 3D nanoemitter. Fig. S3 present the surface morphology of both the bare and AlN-coated InGaN/GaN MQW nanoemitter ordered arrays examined by SEM, respectively. In Fig. S3a,c, it can be seen that the bare sample without AlN coating has a clear 3D surface profile. After depositing 75-cycle AlN by PEALD, each nanopillar is wrapped by a bright region of AlN coating layer in the SEM image of Fig. S3b,d, which is due to the poorer conductivity of AlN than that of Ga(In)N core layers. As a whole, there exhibits the uniform coverage of AlN from top to bottom around 3D ordered array in Fig. S3d.

### **4. The effect of AlN coating layer on the PL light extraction**

AlN has a lower refractive index of 2.035 at 454.3 nm than that of GaN measured by spectroscopic ellipsometer. Its effect on the total light extraction should be further analyzed. Fig. S4 present the schematic diagrams of optical emission path of GaN-based wafer and nanometer-scale pillar with and without AlN coating layer. As for GaN-based wafer, its lateral dimension is much larger than the epitaxial film thickness. There are a part of emitted light beams which may easily induce total internal reflection at the interface of GaN and air in Fig. S4a. Based upon the Snell's law, the critical angle ( $\theta_c$ ) is defined as follow:

$$\theta_c = \arcsin(1/n_f)$$

Where  $n_f$  is the refractive index of the thin film. After depositing the AlN coating layer, the critical angle increases a little from 24.3° to 29.4°. So it may lead to more light beams emitted from the top surface in Fig. S4b. As the deposited AlN layer is quite thin, the increased extraction efficiency is nearly independent on the AlN thickness, which only has a constant improvement of the emitted PL intensity.

On the other hand, nanometer-scale pillar has a high aspect-ratio as shortening the lateral dimension. In Fig. S4c,d, the emission of light beams includes three parts: the top surface, sidewall and bottom surface. The 3D geometrical structure makes the light beams easy to escape out and hence avoids the occurrence of total internal reflection. It has a great advantage in achieving large light-extraction efficiency. By comparison with the GaN-based wafer, coating a thin AlN layer around the nanometer-scale pillar has a much smaller impact on the light extraction.

Besides, it is noted that the main blue PL peak has been enhanced while the defect-related PL peak weakened as increasing the cycle number of AlN coating layer. And it is also worth mentioning that the refractive index has nothing to do with the PL recombination process analyzed in our TRPL results. Therefore, the main PL enhancement, defect-related PL weakening and transient-state PL lifetime as a function of AlN thickness demonstrate that the passivation effect of AlN plays a dominant role rather than its refractive index.

## Figures for supporting information

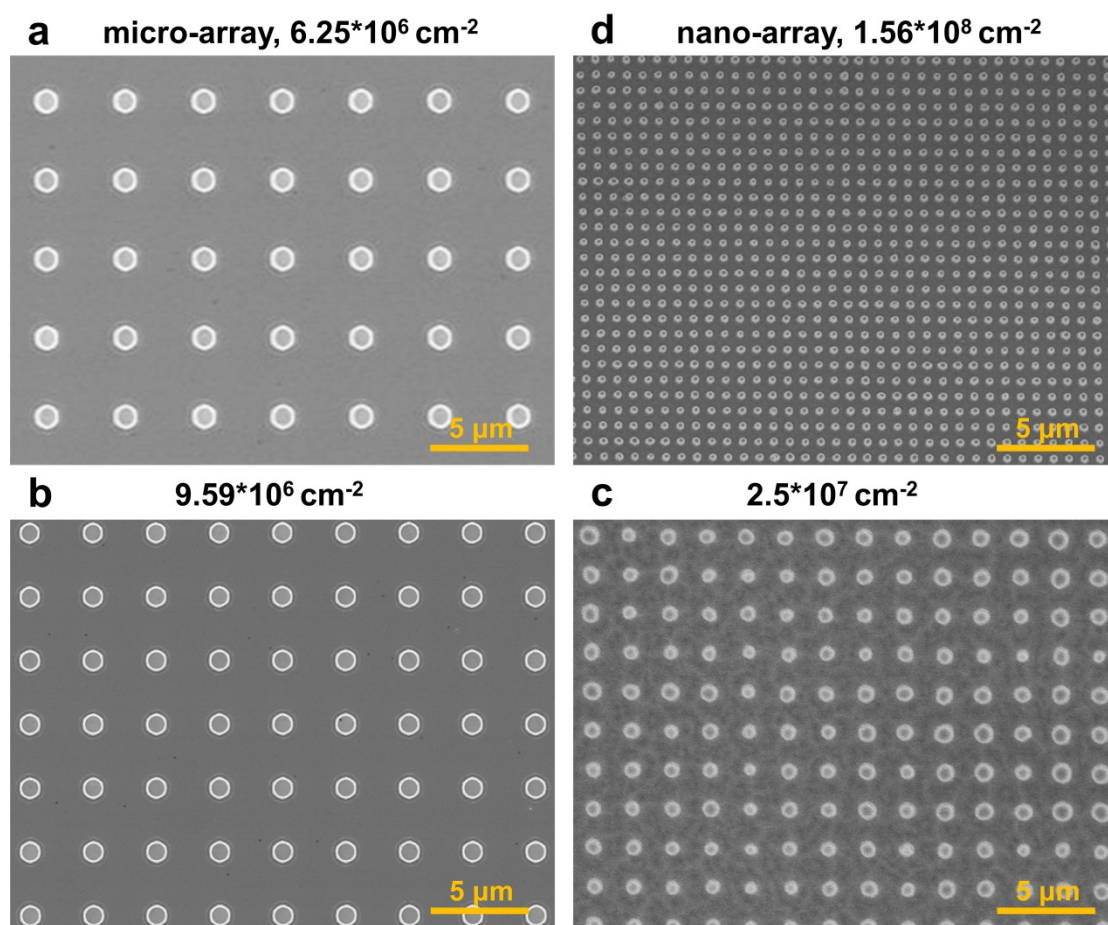


**Fig. S1** Top-down fabricated InGaN/GaN MQW pillar ordered arrays with different pixel densities of (a)  $6.25 \cdot 10^6$ , (b)  $9.59 \cdot 10^6$ , (c)  $2.5 \cdot 10^7$  and (d)  $1.56 \cdot 10^8 \text{ cm}^{-2}$ , respectively.

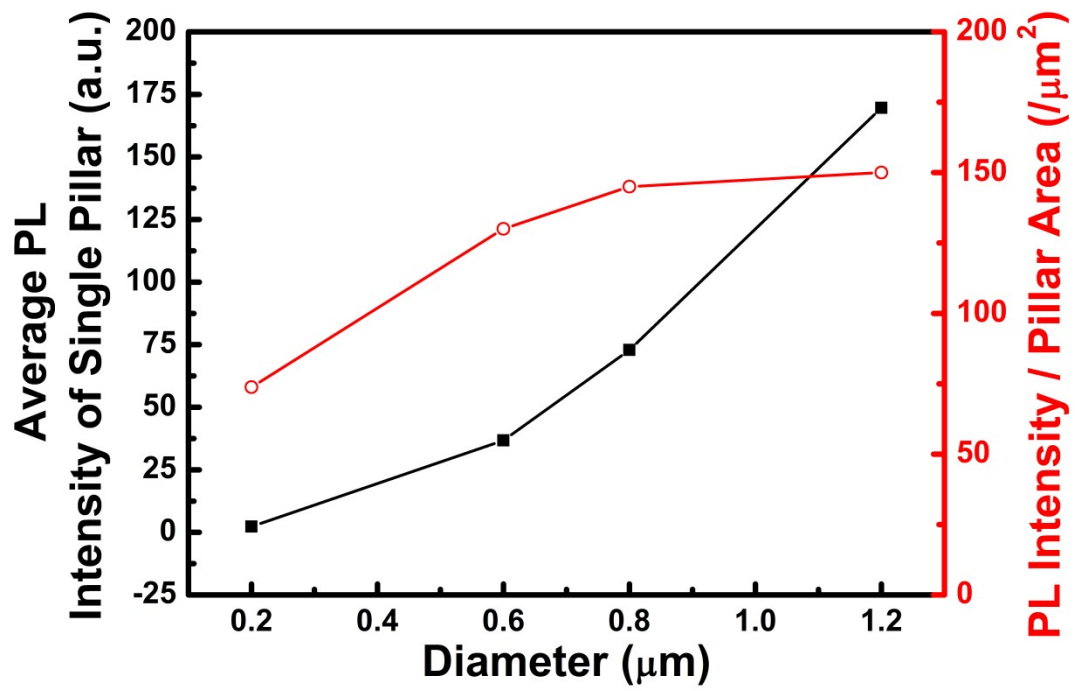
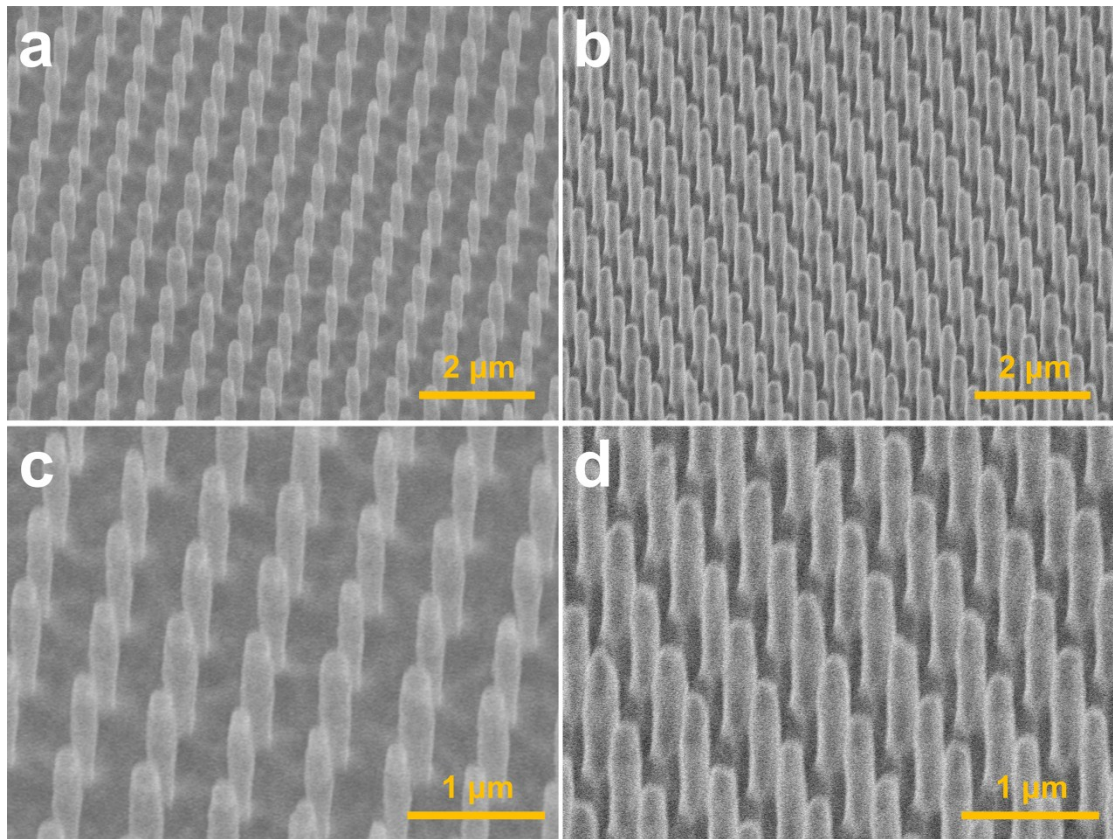
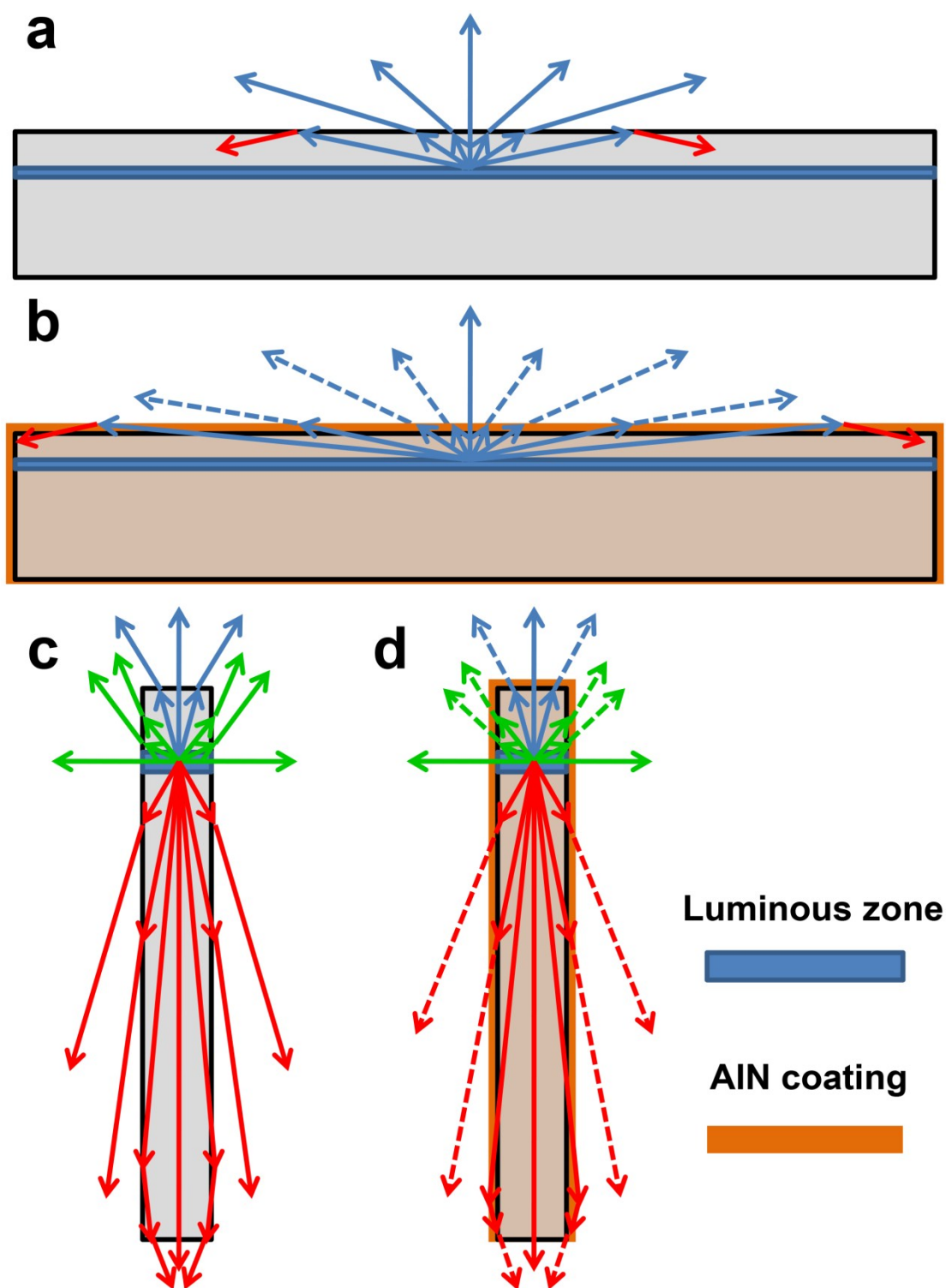


Fig. S2 (a) The average PL intensity and (b) the PL intensity per unit area of PL nanoemitter arrays as a function of the pixel diameter.



**Fig. S3** The SEM images of both the bare (a and c) and AlN-coated (b and d) InGaN/GaN MQW nanoemitter ordered arrays, respectively.



**Fig. S4** The schematic diagrams of optical emission path of (a and b) GaN-based wafer and (c and d) nanometer-scale pillar with and without AlN coating layer, respectively.